J Intell Robot Syst (2014) 76:201–217
DOI 10.1007/s10846-014-0036-7

A Non-Time Based Controller for Load Swing Damping and Path-Tracking in Robotic Cranes

G. Boschetti · R. Caracciolo · D. Richiedei · A. Trevisani

Received: 8 October 2011 / Accepted: 3 February 2014 / Published online: 4 March 2014

Abstract This paper proposes the use of the non-time based control strategy named Delayed Reference Control (DRC) to the control of industrial robotic cranes. Such a control scheme has been developed to achieve two relevant objectives in the control of autonomous operated cranes: the active damping of undesired load swing, and the accurate tracking of the planned path through space, with the preservation of the coordinated Cartesian motion of the crane. A paramount advantage of the proposed scheme over traditional ones is its ease of implementation on industrial devices: it can be implemented by just adding an outer control loop (incorporating path planning) to standard position controllers. Experimental performance assessment of the proposed control strategy is provided by applying the DRC to the control of the oscillation of a cable-suspended load moved by a parallel robot mimicking a robotic crane. In order to implement the DRC scheme on such an industrial robot it has been just necessary to manage path planning and the DRC algorithm on a separate real-time hardware computing the delay in the execution of the desired trajectory suitable to reduce load swing. Load swing has been detected by processing the images from two off-the-shelf cameras with a dedicated vision system. No customization of the robot industrial controller has been necessary.

Keywords Delayed reference control · Swing damping · Coordinated motion · Path tracking · Robotic crane

1 Introduction

Overhead cranes rely on cables for transporting heavy objects in industrial plants. They are widely employed and are usually controlled manually by skilled operators since load swing can damage both the load and the surrounding equipment and may represent a safety issue for plant personnel [1]. The use of autonomous operated automatic cranes, such as robotic cranes [2], imposes therefore the development of effective swing control schemes explicitly addressing the load swing induced by the crane motion and by external disturbances (e.g. impacts), as well as the positioning capability of the system. Although many solutions have been investigated in the recent years (see e.g. [2–16] and the references therein) and some of them have led to industrial applications and commercial

Electronic supplementary material The online version of this article (doi:10.1007/s10846-014-0036-7) contains supplementary material, which is available to authorized users.

G. Boschetti · R. Caracciolo · D. Richiedei ·
A. Trevisani (✉)
Department of Management and Engineering (DTG),
Università degli Studi di Padova, Stradella S. Nicola 3,
36100 Vicenza, Italy
e-mail: alberto.trevisani@unipd.it

diffusion, the design of controllers for the simultaneous path-tracking and swing control of cable suspended loads is still a relevant and open research issue. In literature, both feed-forward (open loop) and feedback (closed loop) control strategies have been proposed.

Feedforward methods are usually based on input shaping techniques (see e.g. [4–6]), which take advantage of the system dynamic model to generate a reference signal that prevents the oscillation before it occurs. Input shaping is simple to implement in real-time controllers. Effective results can however be achieved only if no disturbances affect the system, and if the system natural frequency and damping ratio are accurately known, as well as the suspended load initial conditions (which are usually assumed equal to zero).

Feedback control methods are adopted to overcome such a limitation, at the cost of extra sensors (see e.g. [7–14]). Methods combining feedforward and feedback control techniques have also been proposed (see e.g. [15, 16]). Nevertheless, the techniques relying on feedback control require dedicated controllers, usually high computational efforts, and hence are difficult to implement in existing “closed” industrial controllers.

The aim of this paper is to provide a thorough experimental proof of the effectiveness and ease of implementation of the innovative non-time based active control strategy, referred to as Delayed Reference Control (DRC). Such a feedback technique has been first introduced in [17] and validated in [18] for systems with a single rigid and elastic degree of freedom (dof). Then it has been extended in [19, 20] and [21], and experimentally validated in [14], for systems with an arbitrary number of dofs. The DRC idea has been also successfully exploited in to perform precise synchronous motion control of dual-axis hydraulic systems in the presence of fluid compressibility [22].

The proposed DRC is said a “non-time based” controller since the desired path is expressed as a function of an “action reference parameter” (and not just of the time), which, in turn, is computed on the fly on the basis of the time history of the controlled variables. DRC schemes can be thought of as closed-loop optimal planning schemes, combining the ease of implementation of the optimal motion planning techniques, with the performance robustness with respect to uncertainty and disturbances of the closed-loop controllers.

Two typical and relevant objectives in the control of industrial automatic cranes can be tackled simultaneously by the DRC: the active damping of undesired load oscillations, and the accurate tracking of the robot planned path through space: a strict preservation of the coordinated Cartesian motion of the crane is ensured. In other words the DRC allows reducing load swing while guaranteeing coordinated crane motion even in the presence of unexpected obstacles along the path. These are peculiar features of the DRC, and in particular, the capability of coping with obstacles is a major and apparent advantage over the control methods proposed so far.

Another relevant advantage of the proposed scheme over traditional ones is its ease of implementation on industrial devices: it can be implemented by just adding an outer control loop to standard position controllers. The outer loop, which can be implemented on an external hardware, performs the DRC algorithm and the path generation for the inner position controllers. It is worth mentioning that industrial controllers often allow using external references, while do not admit modifications of the position or speed control schemes, as it would be required by most of the time-based control schemes developed in the literature. Additionally, the implementation of the DRC algorithm requires a small computational effort and therefore real-time control can be performed easily.

In order to highlight the aforementioned strengths, in this work the DRC strategy is applied to reduce the oscillation of a load suspended to the moving platform of an Adept Quattro™ parallel robot by means of a cable. The robot is here employed as a robotic crane and is modelled as a four-dof overhead crane. Only off-the-shelf sensors are employed for real-time swing measurement. In particular, it has been chosen to rely on visual feedback, which is often available in robotic systems (see e.g. [23]). A vision system comprising two cameras and a dedicated image acquisition and processing program (which is coded in C++ by means of the Opensource Computer Vision library) is adopted. The DRC control loop is implemented into a PC running a real-time operative system, and communicating with the robot controller over the Ethernet network and using the UDP protocol.

The paper is organized as follows. In Section 2 the dynamic model of a general four-dof crane is briefly recalled. Section 3 describes the DRC synthesis. Such a control design has been improved with respect to the original one proposed in [19] by proposing a new and more effective method for computing time delays. The experimental set-up and the vision system are discussed in Section 4. The DRC performances in executing two illustrative tasks are shown through experimental results in Section 5. In particular, the DRC capability to cope with the presence of unexpected obstacle within the path is demonstrated. Concluding remarks are finally given in Section 6.

2 Robotic Crane Dynamic Modeling

Let us consider a robotic crane carrying a cable suspended load and forced to move on a single horizontal plane. Whenever the load behaves as a simple pendulum, the system can be modeled through four independent generalized coordinates $\mathbf{p} := \{\theta_X\ \theta_Y\, x\, y\}^T$ Two translations, x and y, describe the planar motion of the robotic crane platform (the trolley) on the XY horizontal plane. Two components of the swing angle $\boldsymbol{\theta} = \left\{ \theta_X\ \theta_Y \right\}^T$ describe the suspended load motion (Fig. 1): θ_X is the swing angle projected on the XZ vertical plane and θ_Y is the swing angle projected on the YZ vertical plane. The definition adopted in this work to represent the swing angle components differs from the one commonly adopted in the modeling of overhead cranes (see e.g. [20]) but is very practical since these angle components are consistent with the angles measured through the vision system developed for the experimental tests (see Section 4).

Hoisting is explicitly neglected in the robotic crane model, as well as the vertical displacement (i.e. the displacement along the Z axis) of the platform.

The suspended load coordinates $\left\{ x_L\ y_L\ z_L \right\}$ are then computed as follows:

$$\begin{cases} x_L = x + h\dfrac{\cos\theta_Y}{\sqrt{1+\tan^2\theta_X+\tan^2\theta_Y}}\tan\theta_X \\ y_L = y + h\dfrac{\cos\theta_X}{\sqrt{1+\tan^2\theta_X+\tan^2\theta_Y}}\tan\theta_Y \\ z_L = -\dfrac{h}{\sqrt{1+\tan^2\theta_X+\tan^2\theta_Y}} \end{cases} \tag{1}$$

where h is the constant cable length.

In order to develop the system dynamic model it has been assumed that the load and the trolley are connected through a massless cable whose stress is tensile and which allows modeling the system through two load sway vibrational modes. Damping has also been neglected, as it is common in practice. Additionally, without loss of generality, it has been assumed that the load mass is concentrated on a single point, and therefore the load moment of inertia (with respect to the load center of mass) has been considered negligible (and therefore no unbalanced large-sized loads leading to a double-pendulum dynamic behavior are considered [5]).

As it is suggested in the original DRC formulation proposed in [19], the synthesis of a DRC scheme can be simplified by taking advantage of linearized system models, rather than directly using nonlinear models. Under the hypothesis that the suspended load has small oscillations about the vertical equilibrium configuration ($\theta_X^{eq} = \theta_Y^{eq} = 0$), the following linearized model allows describing accurately the motion of the system:

$$\begin{bmatrix} h & 0 & 1 & 0 \\ 0 & h & 0 & 1 \\ mh & 0 & M_X+m & 0 \\ 0 & mh & 0 & M_Y+m \end{bmatrix} \begin{Bmatrix} \ddot{\theta}_X(t) \\ \ddot{\theta}_Y(t) \\ \ddot{x}(t) \\ \ddot{y}(t) \end{Bmatrix} + \begin{bmatrix} g & 0 & 0 & 0 \\ 0 & g & 0 & 0 \\ 0 & 0 & 0 & 0 \\ 0 & 0 & 0 & 0 \end{bmatrix} \begin{Bmatrix} \theta_X(t) \\ \theta_Y(t) \\ x(t) \\ y(t) \end{Bmatrix} = \begin{Bmatrix} 0 \\ 0 \\ F_X(t) \\ F_Y(t) \end{Bmatrix} \tag{2}$$

where F_X and F_Y are the platform equivalent driving forces, M_X and M_Y are the equivalent translational masses of the robot platform along respectively the X and Y directions, m is the load mass, g is the gravity acceleration.

The use of linear models is widely employed in literature for the synthesis of both feedback and feedforward control schemes for overhead crane. As a matter of fact, the controlled motion leads to small load oscillations and therefore ensures meeting the linearization

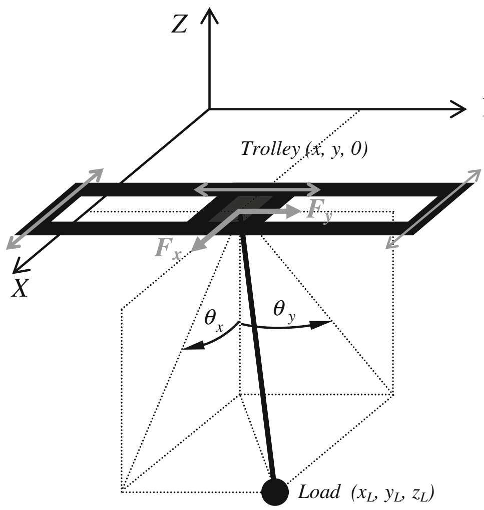

Fig. 1 Scheme of the studied system

hypothesis. Secondly, the direct use of linear models allows reducing the computational effort in the real time solution of the equations of the controller.

The system is clearly underactuated since just two control forces are adopted to perform the simultaneous control of the four system dofs, while no forces are applied directly to the load.

3 DRC Synthesis for a Robotic Crane

The synthesis of a Delayed Reference Controller for a multi-dof system has been first addressed in [19] and will be improved in this work to address the control of a robotic crane. The proposed synthesis takes advantage of the dynamic coupling between the platform absolute displacement $\mathbf{q}(t) = \{x(t), y(t)\}^T$ and the suspended load swing angle $\theta(t) = \{\theta_X(t), \theta_Y(t)\}^T$ shown in (2). Basically, the control action is generated by suitably shifting in time the time history platform reference position $\mathbf{q}^*_{ref}(t)$. The reference hence becomes a function of not just the time, but of a time varying action reference parameter $l \in \Upsilon$ computed on the basis of the measured oscillation (θ_X, θ_Y):

$$\mathbf{q}^*_{ref}(t) = \mathbf{q}_{ref}(l) \tag{3}$$

where $\mathbf{q}^*_{ref}(t)$ is the reference in time, while $\mathbf{q}_{ref}(l)$ is the same variable expressed in the l-domain.

It is therefore assumed that the control problem consists in tracking a desired path through space $\mathbf{q}_{ref}(l)$ rather than a trajectory in time, as in classical control theory. In particular, in DRC schemes l is defined of the form:

$$l = t - \tau \tag{4}$$

and so $\mathbf{q}_{ref}(l) = \mathbf{q}_{ref}(t-\tau)$. The scalar time-varying quantity $\tau \in \mathbb{R}$ is named time delay, even though it can take also negative values. It will be shown that τ allows achieving the desired load swing damping, by suitably shifting in time the robot platform position reference on the basis of the sensed load oscillation, without altering the path through space.

An effective computation of τ can be achieved by focusing on the pendulum-like behavior of the load, described by the first two rows in Eq. (2):

$$\begin{bmatrix} h & 0 \\ 0 & h \end{bmatrix} \begin{Bmatrix} \ddot{\theta}_X(t) \\ \ddot{\theta}_Y(t) \end{Bmatrix} + \begin{bmatrix} g & 0 \\ 0 & g \end{bmatrix} \begin{Bmatrix} \theta_X(t) \\ \theta_Y(t) \end{Bmatrix} = - \begin{Bmatrix} \ddot{x}(t) \\ \ddot{y}(t) \end{Bmatrix} \tag{5}$$

The vector of the platform absolute accelerations on the right hand side of Eq. (5) may be thought of as an equivalent external force $\mathbf{f}$ applied to the load:

$$\mathbf{f}(t) := - \begin{Bmatrix} \ddot{x}(t) \\ \ddot{y}(t) \end{Bmatrix} \tag{6}$$

Clearly, $\mathbf{f}(t)$ may be appropriately set to perform load oscillation control. This goal can be achieved by regulating the time-history of the platform motion. In particular, effective damping of the load oscillations can be obtained whenever the trolley accelerations exciting the load, i.e. $\mathbf{f}(t)$, behave as an active damping force proportional to the actual (or sensed) swing velocities:

$$\mathbf{f}(t) = - \begin{bmatrix} k^\theta_X & k^\theta_{XY} \\ k^\theta_{YX} & k^\theta_Y \end{bmatrix} \begin{Bmatrix} \dot{\theta}_X(t) \\ \dot{\theta}_Y(t) \end{Bmatrix} \tag{7}$$

If Eq. (7) is satisfied, the motion of the trolley controls the load oscillation by providing active damping. On the basis of Eqs. (6) and (7), the DRC synthesis problem is formulated as finding the real scalar τ that allows exerting the desired active damping force while preserving the crane prescribed path through space:

$$\tau \in \mathbb{R} \mid \left\{ \begin{Bmatrix} \ddot{x}(t) \\ \ddot{y}(t) \end{Bmatrix} = \begin{bmatrix} k^\theta_X & k^\theta_{XY} \\ k^\theta_{YX} & k^\theta_Y \end{bmatrix} \begin{Bmatrix} \dot{\theta}_X(t) \\ \dot{\theta}_Y(t) \end{Bmatrix}, \right. \\ \left. \begin{Bmatrix} x(t) \\ y(t) \end{Bmatrix} = \begin{Bmatrix} x_{ref}(t-\tau) \\ y_{ref}(t-\tau) \end{Bmatrix} \right\} \tag{8}$$

Generally speaking, the problem in Eq. (8) has no exact solution. A couple of simplifying hypotheses are then introduced in the DRC synthesis. First of all it is assumed that the tracking error $\mathbf{q}^{*}_{ref}(t) - \mathbf{q}(t)$ can be neglected (i.e. $\mathbf{q}^{*}_{ref}(t) \simeq \mathbf{q}(t)$), and therefore it is assumed that the platform does not alter significantly the trajectory in time calculated to damp the oscillations. This assumption is common in many works proposed in literature, both feedback and feedforward techniques, since industrial controllers usually allow obtaining small tracking errors. This assumption allows replacing the actual platform absolute acceleration with the second derivative of the platform reference position $\ddot{\mathbf{q}}^{*}_{ref}(t)$ in Eq. (5). Secondly, the time history of the crane position reference $\mathbf{q}^{*}_{ref}(t)$ is linearized on the basis of its first-order Taylor's expansion:

$$\mathbf{q}^{*}_{ref}(t) = \mathbf{q}_{ref}(t-\tau) \simeq \mathbf{q}_{ref} - \boldsymbol{\beta}\tau(t) \tag{9}$$

where $\boldsymbol{\beta} = \frac{d\mathbf{q}_{ref}}{dt}$ is the platform reference velocity. The following system of equations approximating problem in Eq. (8) originates therefore from the second derivative of Eq. (9):

$$\boldsymbol{\beta}\ddot{\tau} = -\begin{bmatrix} k_X^{\theta} & k_{XY}^{\theta} \\ k_{YX}^{\theta} & k_Y^{\theta} \end{bmatrix} \begin{Bmatrix} \dot{\theta}_X(t) \\ \dot{\theta}_Y(t) \end{Bmatrix} \tag{10}$$

Equations (8) and (10) show that the control problem is well-posed for any continuous position reference (otherwise delaying the position reference cannot be done), and in the starting and travelling phases of the motion. Therefore, the DRC is mainly aimed at controlling such phases.

Equation (10) is a system made by two linear independent differential equations, with the scalar unknown $\ddot{\tau}$. An unique value of $\ddot{\tau}$ satisfying exactly both equations simultaneously does not exist in the general case. However, a first approximate solution of Eq. (10) can be found by looking for the scalar τ minimizing the square Euclidean norm:

$$\min_{\ddot{\tau}(t)} \left\{ \left\| \boldsymbol{\beta}\ddot{\tau}(t) + \begin{bmatrix} k_X^{\theta} & k_{XY}^{\theta} \\ k_{YX}^{\theta} & k_Y^{\theta} \end{bmatrix} \begin{Bmatrix} \dot{\theta}_X(t) \\ \dot{\theta}_Y(t) \end{Bmatrix} \right\|_2^2 \right\} \tag{11}$$

An extra term $\lambda \|\ddot{\tau}(t)\|_2^2$ should be included in such a minimization problem, in order to prevent the computation of high values of $\ddot{\tau}(t)$, which would lead to high accelerations of the platform, as it can by inferred by the second derivative of Eq. (9). The proposed minimization problem takes therefore the following form:

$$\min_{\ddot{\tau}(t)} \left\{ \left\| \boldsymbol{\beta}\ddot{\tau}(t) + \begin{bmatrix} k_X^{\theta} & k_{XY}^{\theta} \\ k_{YX}^{\theta} & k_Y^{\theta} \end{bmatrix} \begin{Bmatrix} \dot{\theta}_X(t) \\ \dot{\theta}_Y(t) \end{Bmatrix} \right\|_2^2 + \lambda \|\ddot{\tau}(t)\|_2^2 \right\} \tag{12}$$

The scalar positive real value $\lambda \in \mathbb{R}$ allows trading between the cost of missing the control specification in Eq. (11), and the cost of using large values of the control action, which is related to $\|\ddot{\tau}(t)\|_2^2$. The optimal solution of Eq. (12) exists and it can be computed analytically as follows:

$$\ddot{\tau}(t) = -\frac{\boldsymbol{\beta}^T}{\|\boldsymbol{\beta}\|_2^2 + \lambda} \begin{bmatrix} k_X^{\theta} & k_{XY}^{\theta} \\ k_{YX}^{\theta} & k_Y^{\theta} \end{bmatrix} \begin{Bmatrix} \dot{\theta}_X(t) \\ \dot{\theta}_Y(t) \end{Bmatrix} \tag{13}$$

The presence of λ ensures the existence of the solution of the DRC problem, regardless of the values of $\boldsymbol{\beta}$ and of the sensed angles. As a practical rule for the selection of λ, larger values should be selected in case $\|\boldsymbol{\beta}\|_2^2$ approaches zero in order to prevent a swift increase of τ.

Finally, by setting the initial condition $\tau(0) = 0$ and $\dot{\tau}(0) = 0$, the following relation between the delay and the swing angles is established in the time domain:

$$\tau(t) = -\int_0^t \frac{\boldsymbol{\beta}^T}{\|\boldsymbol{\beta}\|_2^2 + \lambda} \begin{bmatrix} k_X^{\theta} & k_{XY}^{\theta} \\ k_{YX}^{\theta} & k_Y^{\theta} \end{bmatrix} \begin{Bmatrix} \theta_X(\psi) \\ \theta_Y(\psi) \end{Bmatrix} d\psi \tag{14}$$

Equation (14) allows computing τ approximating the desired active damping force given by Eq. (7). It clearly shows that the implementation of the proposed regulator in a real-time controller may be performed without incurring significant computational costs. As a matter of fact Eq. (14) just requires some algebraic operations and the integration of the sensed angles. Therefore, Eq. (14) can be easily discretized to allow digital implementation. It is also worth noticing that Eq. (14) does not require the knowledge of the robotic crane equivalent translational masses (M_X and M_Y).

In order to improve the effectiveness of the control action in the presence of nonlinear paths, the impact of the linearization in Eq. (9) upon the DRC performances can be mitigated by computing τ through a time-varying $\boldsymbol{\beta}$ rather than through a constant one. In this way, the nonlinear function representing the reference path is replaced by a sequence of linear functions in the form of Eq. (9) attained through function linearization about the system trajectory. Hence, in general, under the assumption of smooth τ, $\boldsymbol{\beta}$ can be computed as follows:

$$\boldsymbol{\beta}(l) = \left\{ \frac{dx_{ref}(l)}{dl} \;\; \frac{dy_{ref}(l)}{dl} \right\}^T \tag{15}$$

Since an analytical expression of $x_{ref}(l)$ and $y_{ref}(l)$ is usually known in robotic cranes, the analytical expression of $\boldsymbol{\beta}(l)$ is also available, and no numerical derivation is needed. Alternatively, numerical derivation should be employed, which does not represent a severe obstacle in the implementation.

Overall a DRC scheme has a cascade structure consisting in an inner position loop (the standard robotic crane position controller) and an outer swing control loop which includes the trajectory planner and the action reference block. The action reference block is the block computing the action reference parameter $l(t, \theta_X, \theta_Y)$ on the basis of the time variable and the sensed output. Figure 2 schematically depicts such a cascade structure, applied to the robotic crane studied in this work.

The outer control loop is highlighted by adopting double lines. It is apparent that the suggested DRC scheme can be implemented by simply adding an outer loop to any standard position controller, as long as such controllers ensure adequate dynamic responses and therefore negligible tracking error. Clearly, the more the system dynamic behavior meets the hypotheses introduced in the computation of the delay τ, the more load oscillation damping is effective. In real systems, the unavoidable presence of tracking errors and measurement delays, affect the controller performances, by reducing its capability to damp the unwanted oscillation and by decreasing the controlled system phase margin.

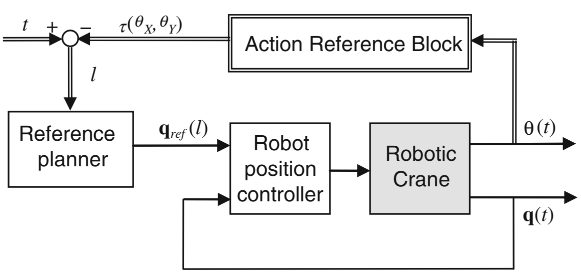

Fig. 2 DRC cascade structure

4 The Experimental Setup

The chief hardware, software, and network components of the experimental setup are schematically depicted in Fig. 3. Such a setup comprises one Adept Quattro industrial robot with its standard real-time controller SmartController CX, a target PC with xPC Target real-time operative system, two firewire CCD cameras, and a dedicated Vision System based on the open source computer vision library called OpenCV. Such a Vision System is running on a PC directly communicating with the target PC.

The Adept Quattro is a four arm "picker"/delta style parallel robot, with a four-dof moving platform (three translations and one rotation about a vertical axis). It is typically employed in industrial pick and place of lightweight objects (see e.g. [24, 25]). In the application proposed in this work the rotation of the moving platform cannot be exploited to reduce load swing and hence it has been neglected. Additionally, in order to make the platform motion recall the one of the trolley of an overhead crane, it has been forced to move on a single horizontal plane.

The suspended load of the robotic crane is connected to the robot platform by means of a nylon cable whose length is 0.95 m. The two swing angle components θ_X and θ_Y are detected by the VS and are measured by observing the slope of the projections of the cable on the camera image planes. Two separate cameras are employed to this purpose. The cameras are fitted perpendicular to each other and with the optical axes parallel to respectively the X and Y axes of the robot reference frame. DRC schemes can however be implemented by assuming any arbitrary sensor or estimation scheme to measure the swing angle. For instance load-cell based observers [26], acceleration-based observers or inclinometers [27] have been proved to be effective and easy-to-be-implemented in industrial environment.

Once the swing angles θ_X and θ_Y are measured, the target PC closes the outer control loop by computing the delay τ through Eq. (14) and by sending to the robot controller the delayed platform reference positions. The software programs on the target PC are uploaded from a host PC running Matlab-Simulink, and implementing the DRC algorithm, with a sampling time of 1 ms.

In order to manage robot motion and external trajectory planning three concurrent real-time tasks

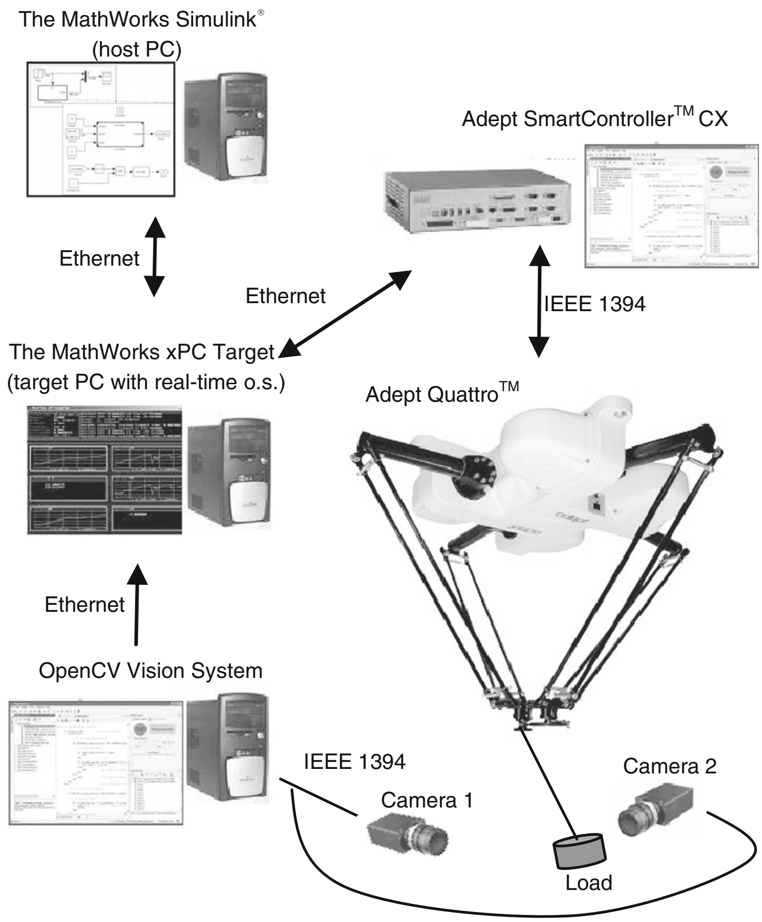

Fig. 3 Scheme (**a**) and picture (**b**) of the chief components of the experimental setup

(threads) run on the robot controller SmartController CX: the *receive communication task*, the *send communication task* and the *control task*. Figure 4 shows the logical scheme of these tasks. The interested reader should refer to [14] for a detailed description of the aforementioned tasks.

The vision system plays a crucial role in the control of the load oscillations since it is employed to measure the two swing angle components of the payload. Slow acquisition rates should be avoided since they reduce the phase margin by introducing delay in the control loop, and therefore downgrade the controller performances. In a previous work [14], the swing angles were measured by means of the Adept Sight Vision System. Such a vision system has allowed achieving some interesting initial results, discussed in the same paper, but the image processing represented a bottleneck of the overall system since it could not operate at a frequency rate higher than 15 Hz. In order to

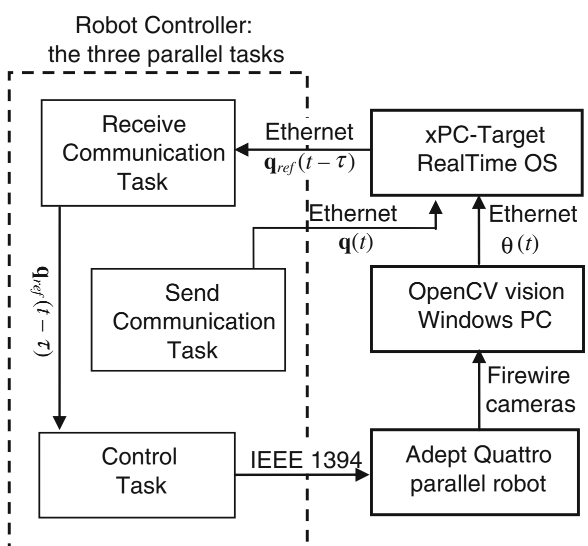

Fig. 4 The Adept Quattro tasks

overcome this limitation a novel vision acquisition and processing system has been developed in this work. The new acquisition process, based on the CMU 1394 Digital Camera Driver. Image processing, has instead been implemented by means of an openCV library capable of performing blob analyses and computing the cable slopes in a time shorter than the frame acquisition time. The number of rows selected (250 rows), which is the parameter most significantly affecting the image processing time, leads to a 60 Hz rate of the feedback signal and a resolution of $4e^{-3}$ rad (3.8 mm in terms of relative linear displacement between the suspended load and the cable attachment point on the moving platform,). Such a resolution is certainly satisfactory for the purposes of the paper.

Finally, the resolution of the images acquired (and in particular the number of columns) combined with the focal length of the camera lead to a measurable workspace of about 200 mm in both the X and Y axes.

5 Experimental Results

The demonstration of the controller peculiar properties and the assessment of its performances are here provided by means of two experimental tests involving two different paths through space:

- a path obtained combining two straight line displacements, leading the suspended load of the crane enter and cross a narrow path confined by vertical "walls" (Fig. 5). The path is broken up by the presence of an obstacle right along the desired path. The obstacle is "unexpected", in the sense that it is not accounted for in motion planning;
- a path combining two harmonic displacements along orthogonal Cartesian directions resulting into a round path with a shape like figure eight: the suspended load is basically required to go around two very close vertical obstacles (Fig. 6).

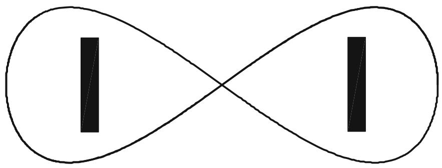

Fig. 6 Scheme of the curved path about two obstacles

The first path consists of two linear paths and is characterized by two corresponding values of $\boldsymbol{\beta}$. In the second experiment, instead, $\boldsymbol{\beta}$ keeps changing and also takes null values. These conditions allow testing the DRC performances under an adequately wide range of operative conditions. Both the experiments demonstrate the capability of the proposed control scheme to improve the robot performances in case the desired motion leads to significant oscillations of the load. The first test also highlights another chief strength of the DRC scheme: if the suspended load hits an obstacle, time delay is made increase indefinitely and hence the load is stopped until the obstacle is removed. Such a feature might be interestingly exploited to improve robotic crane operational safety.

Basically, the experiments aim at proving that the DRC regulator can suitably shift the execution of the desired trajectory in time, rather than showing that minimum load oscillations can be achieved: heuristic rules have been therefore adopted to tune the controller gains, and no trial-and-error optimization has been performed. A simple rule has been followed to set the equivalent damping force (i.e. the controller gains k_X^θ, k_Y^θ, k_{XY}^θ, k_{YX}^θ), in order to show that effective results can be attained without performing time-consuming tuning. It consists in choosing

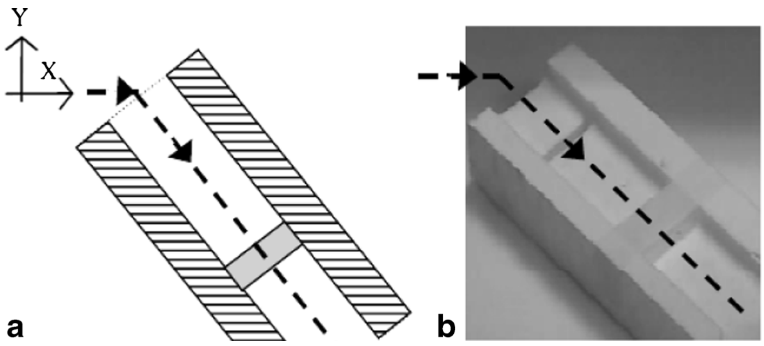

Fig. 5 Scheme (**a**) and picture (**b**) of the piecewise straight path with obstacle and picture (**b**) of the object employed to confine the path

decoupled equivalent forces (i.e. $k^{\theta}_{XY} = k^{\theta}_{YX} = 0$) that ensure achieving the desired equivalent damping ratio (ξ_{DES}) of the oscillating load dynamics. In particular, the equations from (5) to (7) can be rearranged to get the following closed loop decoupled load swing dynamics:

$$\begin{cases} h\ddot{\theta}_X + g\theta_X = -k^{\theta}_X\dot{\theta}_X \\ h\ddot{\theta}_Y + g\theta_Y = -k^{\theta}_Y\dot{\theta}_Y \end{cases} \tag{16}$$

and hence, the gains of the DRC can be computed as follows:

$$k^{\theta}_X = k^{\theta}_Y = 2\xi_{DES}\sqrt{hg} \tag{17}$$

In particular, the results shown in this Section have been attained by imposing $\xi_{DES} = 1$ in Eq. (17). Other approaches can be followed to obtain non diagonal or asymmetric matrices: as an example, matrix $\begin{bmatrix} k^{\theta}_X & k^{\theta}_{XY} \\ k^{\theta}_{YX} & k^{\theta}_Y \end{bmatrix}$ could be obtained as the solution of a Linear Quadratic Control problem. Clearly, a fine tuning of the parameters would yield a regulator with better performances in terms of oscillation damping. However, this goes beyond the aims of the paper.

The term λ has been set to 10^{-4} in the first test, while it has been set to 10^{-2} in the second test. Such a difference is mainly motivated by the need of coping with the null values taken by $\boldsymbol{\beta}$ along the second path: by reducing λ it is possible to mitigate the effect of $\|\boldsymbol{\beta}\|_2$ in the computation of τ, at the expense of a reduction in the control promptness in damping oscillations.

For all the tests carried out, a comparison is proposed between the performance attained with and without DRC.

5.1 Test 1: Piecewise Linear Straight Line Path Confined by Walls, with Obstacle

Two objectives are to be pursued by the sequence of linear paths assumed as the first test. On the one hand, such a path is useful to assess the damping capabilities of the DRC when relevant load oscillations are introduced by the step changes in the first derivative of the undelayed position reference. On the other, it clearly shows the peculiar behavior of the DRC in the presence of unexpected obstacles along the path.

Figure 5a sketches the theoretical path that should be followed by the load (dotted black line), the walls confining the path and the obstacle obstructing the motion. Figure 5b shows a picture of the objects used to mimic the obstacle and the walls confining the middle part of the path. The coordinates of the points adopted to define the path are collected in Table 1, where they are expressed in the robot world reference frame. The suspended load should first enter the area where there are the walls by following a very short straight line path (from start point to via point 1). It should then move parallel to the walls following a straight line path different form the first one. Finally, it hits an unexpected obstacle (simulated by an adhesive tape fixed to the two walls, as it is shown in Fig. 5b and in Fig. 7) which is placed along the straight line path between via point 1 and the end point. In particular, Fig. 7 shows some snapshots of experimental tests, without (first row of pictures) and with (second row) DRC. The arrows show the direction of motion of the load in each picture. Their lengths just provide an intuitive idea of the load velocity. The differences between behaviors in the two tests can be easily compared in Online Resource 1.

Some relevant recordings of this test are shown in the figures from 8 through 12. The results refer to a sample test, among several repetitions of the same path performed. Indeed, the repetition of the path more than once leads to almost identical results. As a matter of fact, DRC control schemes preserve their effectiveness even in the presence of unknown and not null displacement and velocity initial conditions, as it has been demonstrated in [14]. Figure 8 displays the time histories of the position references along the Cartesian axes *X* and *Y*, both when the DRC is employed in the outer control loop (the delayed references, straight line) and when it is not (the undelayed references, dotted line). It clearly shows how the DRC outer loop shapes the platform planned motion for damping the load oscillation. The references have been delayed in time by the values of τ computed in accordance with Eq. (14) and plotted in Fig. 9. Figure 9 also displays the consequential time history of l.

Table 1 Coordinates of the points through which the piecewise straight line path has been defined

Start point: ($x = 22.5$ mm, $y = 0$, $z = 0$)
Via point 1: ($x = 47$ mm, $y = 0$, $z = 0$)
End point: ($x = 212.5$ mm, $y = 167$ mm, $z = 0$)
Undelayed reference velocities $v_x = 60$ mm/s $v_y = -60$ mm/s

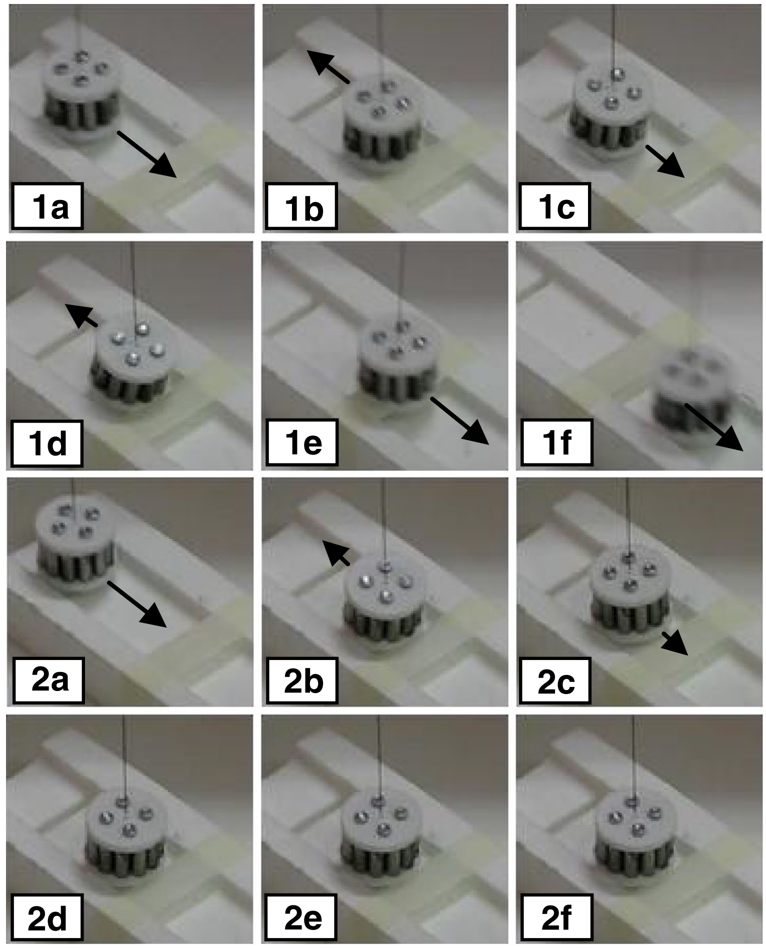

Fig. 7 Snapshots of the path broken up by an obstacle (row "1": without DRC; row "2": with DRC)

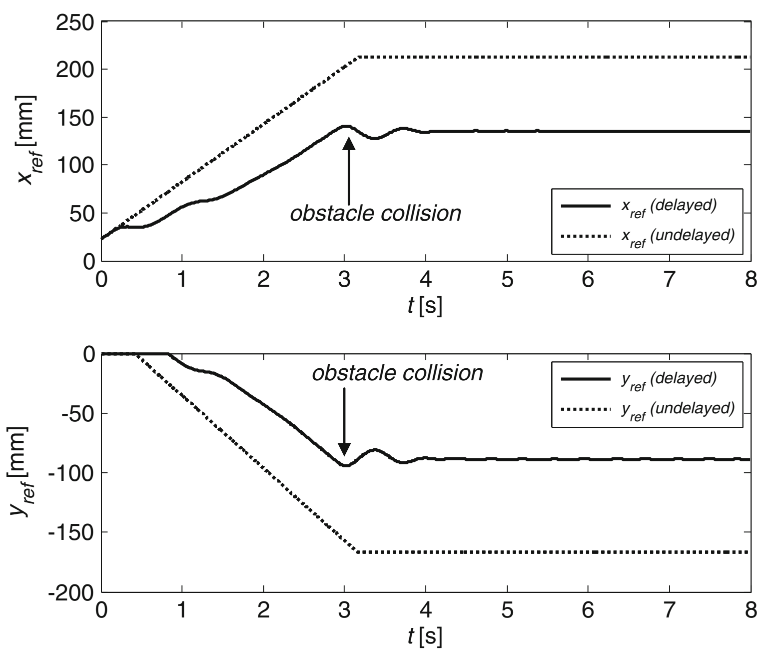

Fig. 8 Robot platform position references in the X and Y directions vs. t

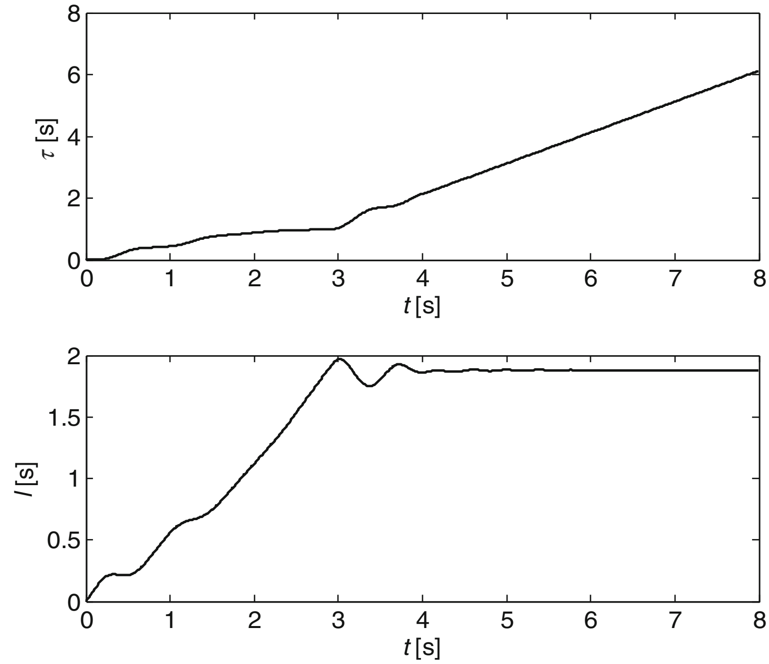

Fig. 9 τ vs. t and l vs. t, with the DRC control scheme

It is worth mentioning that the basic DRC proposed in this paper does not allow preventing impacts, since neither structured environment or obstacle detection systems are assumed. Nonetheless, the peculiar feature of DRC to slow down and, in the end, to stop the motion in the presence of impacts allows smoothing

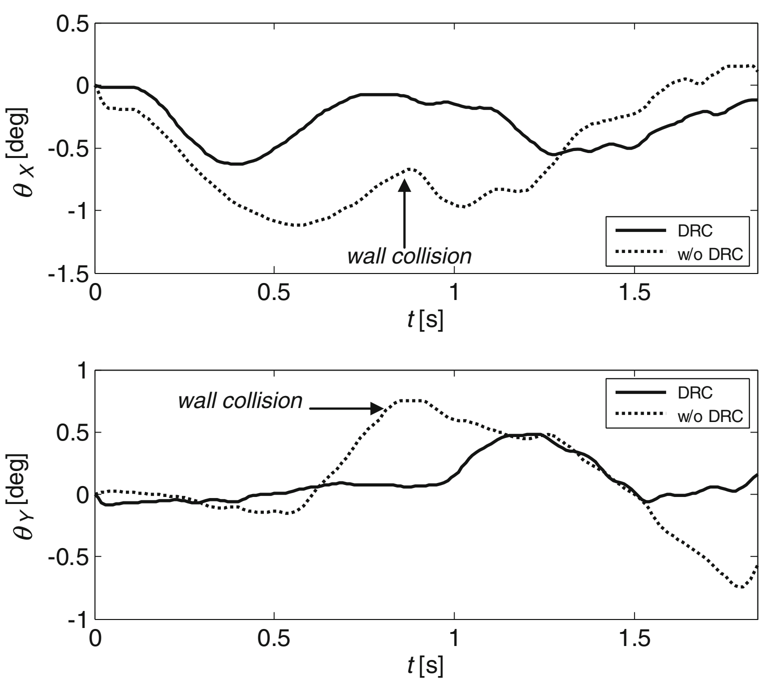

Fig. 10 Detail of the swing angle components before the collision

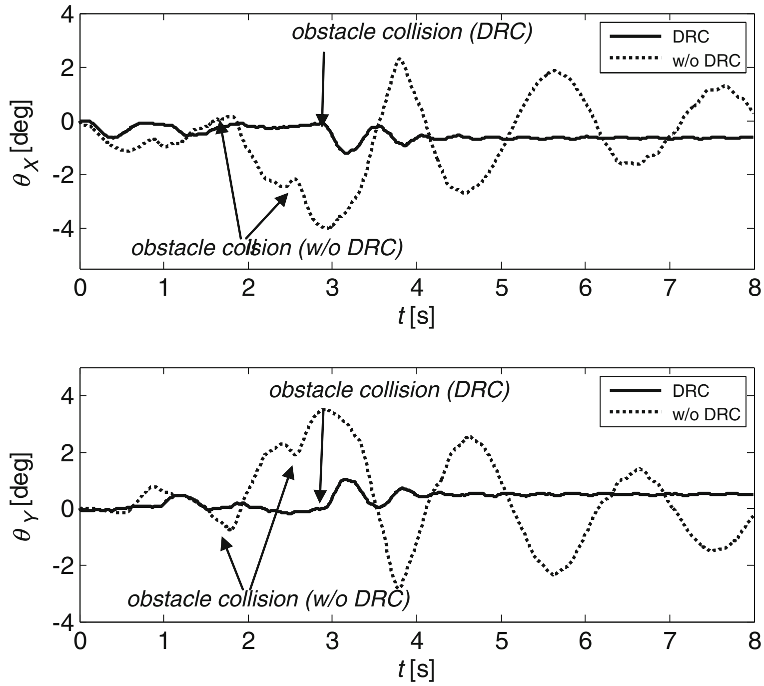

Fig. 11 Swing angle components vs. t

the impacts themselves and reducing damages whenever obstacle avoidance systems are not available or fail.

Figure 10 shows a detail of the time histories of the measured swing angle components, before the collision with the obstacle occurs. By comparing Figs. 9 and 10, it can be recognized that the DRC makes τ promptly increase at the time instants ($t = 0.2$ s and $t \simeq 1$ s) when the platform motion originates swift variations of $\boldsymbol{\theta}$. Afterwards τ rises at a lower rate and almost approaches steady values (see e.g. from $t = 0.65$ s to $t \simeq 1$ s, and from $t \simeq 2.5$ s to

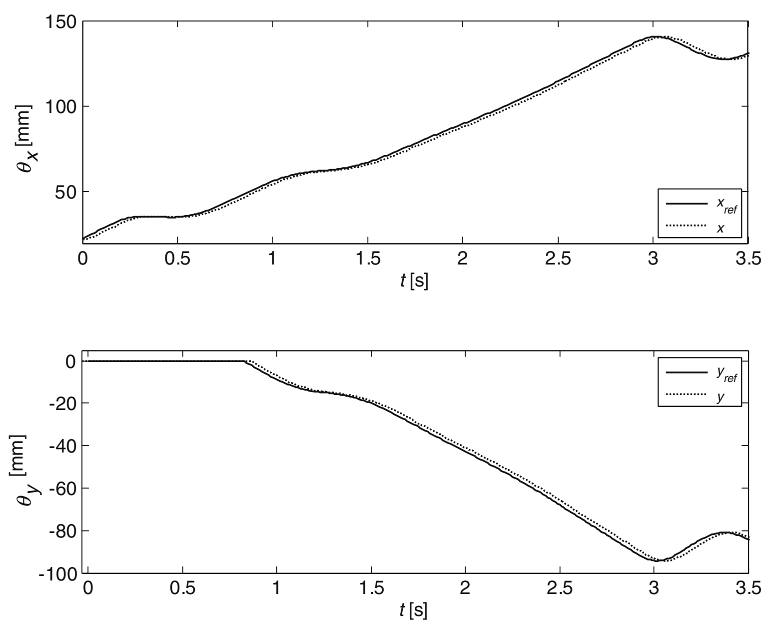

Fig. 12 Details of the robot platform reference and actual positions in the X and Y directions vs. t

$t \simeq 3$ s). Figure 10 clearly proves that the DRC ensures an adequate damping of the suspended load oscillation. Conversely, frequent collisions with the walls confining the path occur in case the sole inner position loop is employed, i.e. when the DRC is not running (see e.g. $t \simeq 0.85$ s).

Figure 11 provides the full experimental recordings of the swing angle components, and therefore it shows the effects of the collision with the obstacle (details 1B and 2B, Fig. 7), which significantly excites load oscillations. In particular, without DRC the robot obviously keeps moving the load after the collision with the obstacle. Even if the load motion is obstructed by the obstacle, the robot strives to pull the load, by making it tilt (1D) and then cross the obstacle (1E), with resulting uncontrolled large amplitude oscillations (1F). This can lead to easily conceivable consequences when the obstacles or the load are of hazardous or fragile nature. On the contrary, after the collision the DRC keeps the reference position almost constant (see Fig. 8, $t \simeq 3$ s) because such a disturbance causes increases of the load angles which cannot be compensated without drifting away from the desired path. This result is a consequence of the fact that τ increases at the same rate as t and therefore l takes constant values (see Fig. 9). Since the desired equivalent damping force $\mathbf{f}(t)$ is a function of the swing velocities, the DRC allows avoiding any increase or oscillation of the swing angles. Constant values of the angle components are therefore attained. The small amplitude transient oscillations are just consequences of the elasticity of the obstacle material.

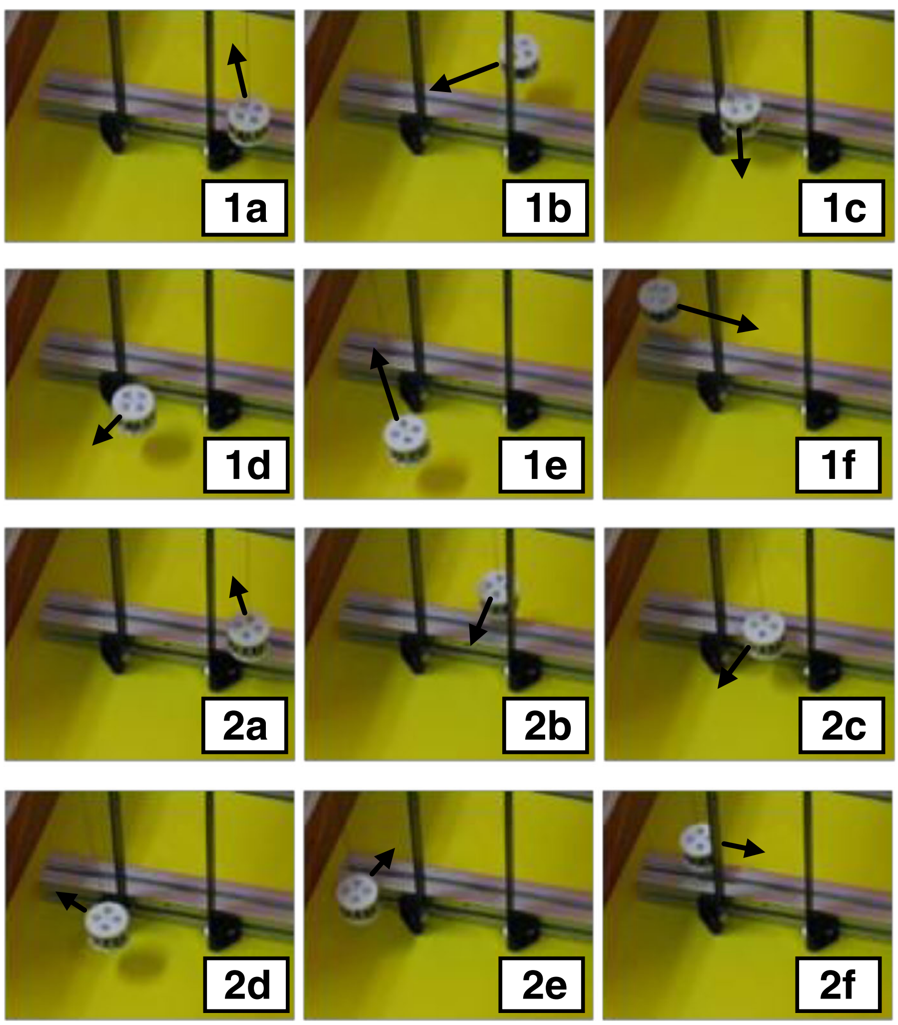

Fig. 13 Snapshots of the curved path around two obstacles (row "1": without DRC; row "2": with DRC)

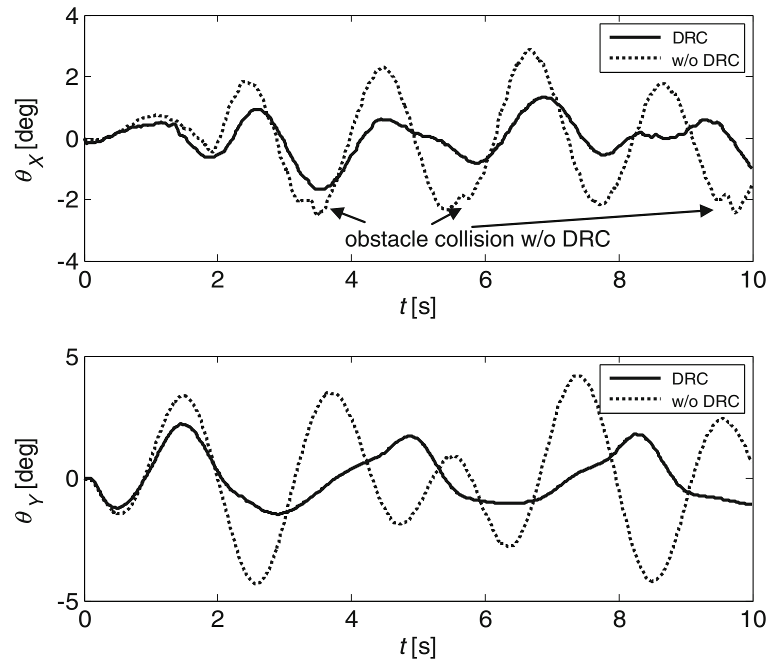

Fig. 14 Swing angle components vs. t

The same behaviour is evident in the snapshots provided in Fig. 7: after a short transient, when the load bounces back because of the impact with the elastic obstacle (2B), the DRC swiftly controls the load by keeping it at a constant position (2D, 2E, 2F). The platform motion along the planned path leading to such a result can be more clearly caught in Online Resource 2.

The usefulness of this DRC feature in improving robotic crane operational safety is evident.

Finally, Fig. 12 shows the position tracking error (tracking lag) by comparing the reference and the actual value of the robot platform positions in both the X and Y axes. The proposed results refer to the control performed in the presence of the DRC. Yet, a similar behavior is attained in the presence of the sole inner

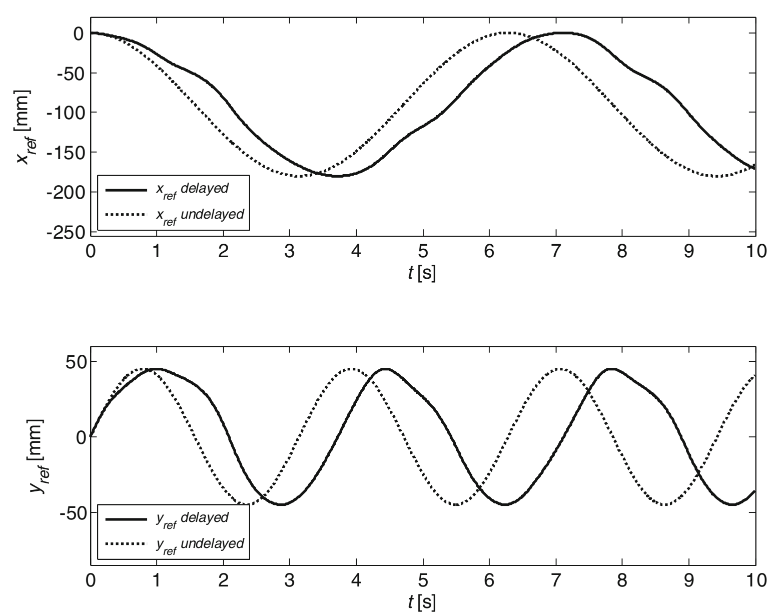

Fig. 15 Robot platform position references in the X and Y directions vs. t

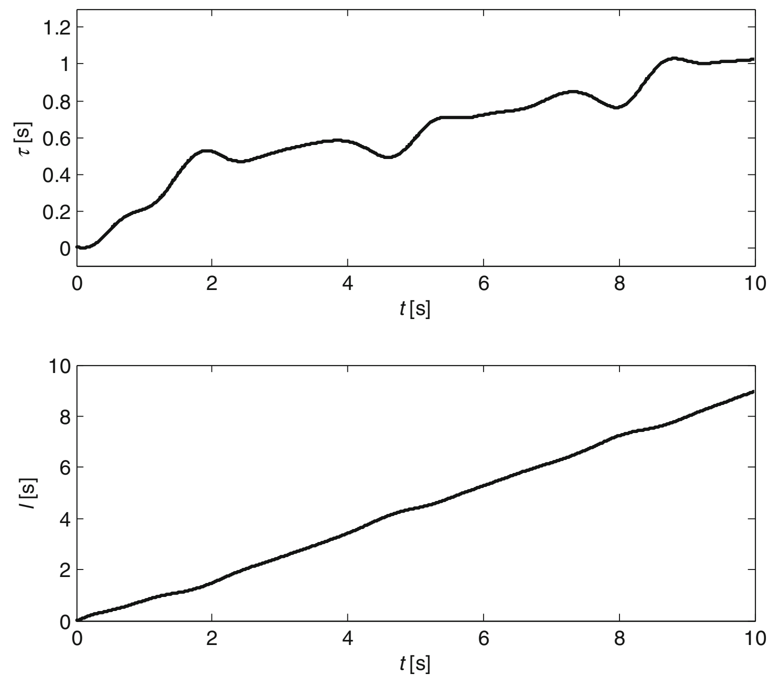

Fig. 16 τ vs. t and l vs. t, with the DRC control scheme

position loop. Clearly, such a result does not allow fully meeting the requirement of a negligible position tracking error, and decreases the controller effectiveness. A reduction of the tracking lag, as well as a further reduction of the swing angle acquisition and computational time would certainly lead to even better performances of the DRC.

5.2 Test 2: Curved Path Around Two Obstacles

Ever changing and also null values of $\boldsymbol{\beta}$ characterize the second curved path. It is here assumed that the suspended load needs to go around two obstacles by following a path basically recalling the shape of the number "8", as it is sketched in Fig. 6. A collection of some snapshots of experimental tests carried out with (row 2) and without (row 1) DRC is proposed in Fig. 13, while the video recording of the two tests is shown in Online Resource 3.

In detail, the robot platform position reference defined in the X and Y axes are respectively:

$$\begin{cases} x_{ref}(l) = 90\,(cos\,(l) - 1) \\ y_{ref}(l) = 45 sin\,(2l) \end{cases} \quad [\text{mm}] \tag{18}$$

Lack of oscillation control leads to unavoidable collisions between the load and the obstacles (see picture 1C in Fig. 13). This is also confirmed by the time histories of the load swing angle components which are shown in Fig. 14. The DRC scheme can considerably reduce the load unwanted oscillations and prevent collisions.

Only a small residual low frequency oscillation due to the centrifugal effect can be observed. Such an oscillation is orthogonal to the path and arises whenever curved paths are tracked, and therefore it cannot be compensated being the system underactuated. Finally, Fig. 15 compares the robot platform position references in the Cartesian axes, while Fig. 16 shows the time histories of τ and l. Overall, the latter highlights that just a small delay is needed to get an effective suppression of the unwanted load oscillations at the swing natural frequency and to prevent collisions.

6 Conclusions

This paper introduces an improved version of the Delayed Reference Control (DRC) for the swing control of a robotic crane and proves its effectiveness and industrial-oriented design through a set of significant experiments carried out on an industrial test rig.

The effectiveness of the scheme is assessed by showing the experimental recordings from two challenging tasks involving different paths through space. The consequences of collisions with unexpected obstacles are also shown and discussed. Overall, the shift in time of the trajectories caused by the DRC are shown to lead to significant decreases to the oscillations of the suspended load. Additionally, contrary to many traditional time-based regulators, the coordinated Cartesian motion of the robotic crane is always assured.

The assessment of the DRC effectiveness has been carried out on an experimental setup comprising an industrial robot mimicking a robotic crane: this choice makes apparent how easy it is to implement DRC schemes on industrial devices. This is basically a consequence of the low computational effort required to calculate the time delay and of the fact that its implementation just compels closing an outer swing control loop outside the standard inner position controller of the robotic crane. Such an outer loop includes the path planner generating the references for the inner loop, and the DRC algorithm computing the suitable time delay leading to the desired equivalent damping force. The calculation of the time delay just compels the direct measurement of the load swing angle components. In the experiments it has been chosen to rely on visual feedback provided by off-the-shelf cameras, which is often available in robotic systems. Though commercial software could be employed to perform image acquisition and processing, in this work a software program employing open-source libraries has been developed, to achieve higher feedback rate and measurement resolution.

References

1. Martínez-Salvador, B., Pérez-Francisco, M., Del Pobil, A.P.: Collision detection between robot arms and people. J. Intell. Robot. Syst. **38**, 105–119 (2003)
2. Lew, J.Y., Khalil, A.: Anti-swing control of a suspended load with a robotic crane. In: Proceedings of the ACC, pp. 1042–1046, Chicago, USA (2000)
3. Abdel-Rahman, E.M., Nayfeh, A.H., Masoud, Z.N.: Dynamics and control of cranes: a review. J. Vib. Contr. **9**(7), 863–909 (2003)
4. Blackburn, D., Lawrence, J., Danielson, J., Singhose, W., Kamoi, T., Taura, A.: Radial-motion assisted command shapers for nonlinear tower crane rotational slewing. Control. Eng. Pract. **18**, 523–531 (2010)
5. Vaughan, J., Kim, D., Singhose, W.: Control of tower cranes with double-pendulum dynamics. IEEE Trans. Contr. Syst. Technol. **18**(6), 1345–1358 (2010)
6. Singer, N.C., Seering, W.P.: Preshaping command inputs to reduce system vibration. J. Dyn. Syst. Meas. Contr. **112**(1), 76–82 (1990)
7. Bowling, D., Starr, G., Wood, J., Lumia, R.: Wide band suppression of motion-induced vibration. In: Proceedings of the IEEE International Conference on Robotics and Automation. Rome (2007)
8. Hong, K.-S., Ngo, Q.H.: Port automation: modeling and control of container cranes. In: Proceedings of International Conference on Instrumentation, Control & Automation. Bandung (2009)
9. Kim, C.-S., Hong, K.-S.: Boundary control of container cranes from the percpective of controlling an axially moving string system. Int. J. Contr. Autom. Syst. **7**(3), 437–445 (2009)
10. Klosinski, J.: Swing-free stop control of the slewing motion of a mobile crane. Contr. Eng. Pract. **13**, 451–460 (2005)
11. Hong, S.-W., Bae, G.-H., Kim, B.-G.: Development of miniature tower crane and payload position tracking system using web-cam for education. In: Proceedings of IASTED International Conference on Robotics and Applications. Cambridge (2010)
12. Yang, J.H., Shen, S.H.: Novel approach for adaptive tracking control of a 3-D overhead crane system. J. Intell. Robot. Syst. **62**, 59–80 (2011)
13. O'Connor, W.J.: A gantry crane problem solved. ASME. J. Dyn. Syst. Meas. Contr. **125**(4), 569–576 (2003)
14. Boschetti, G., Richiedei, D., Trevisani, A.: Delayed reference control for multi-degree-of-freedom elastic systems: theory and experimentation. Contr. Eng. Pract. **19**, 1044–1055 (2011)
15. Schaub, H.: Rate-based ship-mounted crane payload pendulation control system. Contr. Eng. Pract. **16**, 132–145 (2008)
16. Sorensen, K.L., Singhose, W., Dickerson, S.: A controller enabling precise positioning and sway reduction in bridge and gantry cranes. Contr. Eng. Pract. **15**, 825–837 (2007)
17. Gallina, P., Trevisani, A.: Delayed reference control of a two mass elastic system. J. Vib. Contr. **10**, 135–159 (2004)
18. Gallina, P., Trevisani, A.: Synthesis and experimental validation of a delayed reference controller for active vibration suppression in mechanical systems. J. Appl. Mech.-T. ASME **72**, 623–627 (2005)
19. Richiedei, D., Trevisani, A.: Design of delayed reference controllers for simultaneous path tracking and active vibration damping of multi-degree-of-freedom linear systems. J. Vib. Contr. **15**(3), 323–346 (2009)
20. Caracciolo, R., Boschetti, G., Richiedei, D., Trevisani, A.: Moving the suspended load of an overhead crane along a pre-specified path: a non-time based approach. Robot. Comput. Integrat. Manuf. **30**(3), 256–264 (2014)
21. Boschetti, G., Richiedei, D., Trevisani, A.: Delayed reference control applied to flexible link mechanisms: a scheme for effective and stable control. J. Dyn. Syst. Meas. Control-T. ASME **134**(1), 011003.1–011003.9 (2012)

22. Richiedei, D.: Synchronous motion control of dual-cylinder electrohydraulic actuators through a non-time based scheme. J. Contr. Eng. Appl. Informat. **14**(4), 80–89 (2012)
23. Yoshida, Y., Tabata, H.: Visual feedback control of an overhead crane and its combination with time-optimal control. In: Proceedings of the IEEE/ASME International Conference on Advanced Intelligent Mechatronics. Xi'an (2008)
24. Pierrot, F., Nabat, V., Company, O., Krut, S., Poignet, F.: Optimal design of a 4-DOF parallel manipulator: from academia to industry. IEEE Trans. Robot. **25**(2), 213–24 (2009)
25. Boschetti, G., Rosa, R., Trevisani, A.: Optimal robot positioning using task-dependent and direction-selective performance indexes: general definitions and application to a parallel robot. Robot. Comput. Integrat. Manuf. **29**(2), 431–443 (2013)
26. Ebrahimi, M., Ghayour, M., Madani, S.M., Khoobroo, A.: Swing angle estimation for anti-sway overhead crane control using load cell. Int. J. Contr. Automat. Syst. **9**(2), 301–309 (2011)
27. Kim, Y.S., Hong, K.S., Sul, S.K.: Anti-sway control of container cranes: inclinometer, observer, and state feedback. Int. J. Contr. Automat. Syst. **2**(4), 435–449 (2004)